can apparently account for 1.3 kcal/mol of this decrease (Figure 2).[29] Similar medium effects may modulate the stability of planar peptide bonds during the folding,[1,2] function,[30] or lysis[28] of proteins.

Acknowledgment. We thank Dave Quirk, Phil Hajduk, Dave Horita, Yijeng Liu, Kim Dirlam, and the staff at NMRFAM [Grant RR02301 (NIH)] for their assistance and Professors Sam Gellman and George Reed for helpful discussions. E.S.E. is a Wharton Predoctoral Fellow. S.N.L. is supported by Cellular and Molecular Biology Training Grant GM07215 (NIH). A.P.H. is supported by Molecular Biophysics Training Grant GM08293 (NIH). R.T.R is a Presidential Young Investigator (NSF), Searle Scholar (Chicago Community Trust), and Shaw Scientist (Milwaukee Foundation).

Supplementary Material Available: Figures showing the ^{13}C NMR spectrum of **1** ($CDCl_3$) and IR spectrum of Ac-Pro-OMe (aqueous) and a table listing activation parameters for isomerization of **1** in all solvents studied (4 pages). Ordering information is given on any current masthead page.

(29) Since the free energy of desolvation of a proline residue is 3.0 kcal/mol (Gibbs, P. R.; Radzicka, A.; Wolfenden, R. *J. Am. Chem. Soc.* **1991**, *113*, 4714–4715), desolvation destabilizes by 1.7 kcal/mol the transition state for prolyl peptide bond isomerization. Interactions (such as hydrogen bonds) may stabilize by 6.7 kcal/mol an orthogonal transition state in the active sites of the PPIases. For a discussion of the manifestation of binding energy in enzymatic catalysis, see: Hansen, D. E.; Raines, R. T. *J. Chem. Educ.* **1990**, *67*, 483–489.

(30) (a) Dunker, A. K. *J. Theor. Biol.* **1982**, *97*, 95–127. (b) Gerwert, K.; Hess, B.; Engelhard, M. *FEBS Lett.* **1990**, *261*, 449–454. (c) Williams, K. A.; Deber, C. M. *Biochemistry* **1991**, *30*, 8919–8923.

Correlation of Electrode Surface Structure with Activity toward H_2O_2 Electroreduction for Bi Monolayers on Au(111)

Chun-hsien Chen and Andrew A. Gewirth*

Department of Chemistry
University of Illinois at Urbana–Champaign
505 South Mathews Aveune, Urbana, Illinois 61801

Received April 2, 1992

We present in situ atomic force microscope (AFM) images of two different structures of Bi underpotentially deposited[1] (upd) on Au(111). The two different structures are correlated with the activity of this surface toward the electroreduction of H_2O_2 to H_2O in acid electrolyte.

The upd of Bi on Au(111) has been well studied because the Bi overlayer acts as a catalyst for electroreduction processes.[2–4] The electrocatalytic activity of this surface is known to be dependent on the coverage of Bi. Three distinct stages in reactivity as a function of potential (and hence Bi coverage) have been observed.[3] Electrodes with intermediate coverage of Bi are significantly more active toward reduction of H_2O_2 than either the full monolayer-covered surface or the bare Au(111). The Bi on Au system has been intensively studied, and general voltammetric response,[3,5–7] electrosorption valency,[8–11] correlation between charge and structure,[12,13] desorption kinetics,[14,15] surface conductivity,[16] and specular reflectivity[9,17] have all been examined. However, there is no direct insight available into the structures present on the surface, nor to the structural changes responsible for the changes in electrocatalytic activity. In order to understand the catalytic process, detailed in situ studies of the upd structures are necessary.

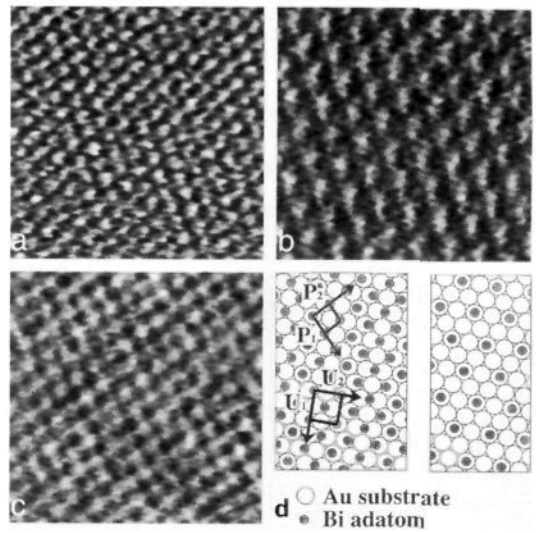

Figure 1. AFM images (5 × 5 nm) of Bi upd on Au(111) in 0.1 M $HClO_4$. (a) Au(111) surface found positive of Bi upd peaks. Atom–atom distance is 0.29 nm. (b) (2 × 2)-Bi adlattice found at 200 mV vs $E_{Bi^{3+/0}}$. Atom–atom distance is 0.57 ± 0.02 nm. (c) Uniaxially commensurate, rectangular Bi adlattice found at 100 mV. Atom–atom distance is 0.34 ± 0.02 nm. (d) Schematic of Bi structures: left, rectangular lattice where **P** and **U** are primitive and nonprimitive unit cell vectors, respectively; right, (2 × 2)-Bi adlattice showing open Au and Bi sites. The Bi adatoms are larger than Au; they are shown smaller here for clarity.

Figure 1a shows the AFM image obtained in 1 mM Bi^{3+} + 0.1 M $HClO_4$ at potentials positive of the first Bi upd peak, which occurs at 360 mV.[18] This lattice exhibits a hexagonal orientation and 0.29 ± 0.02 nm atom–atom spacing which corresponds to the bare Au(111) surface. When the potential is moved to between 250 and 190 mV, an overlayer of Bi atoms forms (Figure 1b). This upd overlayer is an open, hexagonal structure with an atom–atom spacing of 0.57 ± 0.02 nm, which is 2 times the Au spacing. This lattice exhibits <5° rotation relative to the Au lattice and is thus equivalent to a (2 × 2)-Bi commensurate structure. The right side of Figure 1d shows one arrangement of this (2 × 2)-Bi lattice; other arrangements with the Bi in 3-fold hollow or bridging sites are also possible.

* To whom correspondence should be addressed.

(1) Kolb, D. M. In *Advances in Electrochemistry and Electrochemical Engineering*; Gerischer, H., Tobias, C. W., Eds.; Wiley: New York, 1978; Vol. 11, pp 125–271.

(2) Adzic, R. In *Advances in Electrochemistry and Electrochemical Engineering*; Gerischer, H., Tobias, C. W., Eds.; Wiley; New York, 1984; Vol. 13, pp 159–260.

(3) Sayed, S. M.; Juttner, K. *Electrochim. Acta* **1983**, *28*, 1635–1641.

(4) Adzic, R. R.; Markovic, N. M.; Tripkovic, A. V. *Glas. Hem. Drus. Beograd* **1980**, *45*, 399–409.

(5) Schmidt, E.; Gygax, H. R.; Cramer, Y. *Helv. Chim. Acta* **1970**, *53*, 649–654.

(6) Cadle, S. H.; Bruckenstein, S. *J. Electrochem. Soc.* **1972**, *119*, 1166–1169.

(7) Martins, M. E.; Galindo, M. C.; Arvia, A. *An. Quim.* **1990**, *86*, 327–336.

(8) Schmidt, E.; Beutler, P.; Lorenz, W. J. *Ber. Bunsenges. Phys. Chem.* **1971**, *75*, 71–78.

(9) Adzic, R.; Jovancicevic, V.; Podlavicky, M. *Electrochim. Acta* **1980**, *25*, 1143–1146.

(10) Deakin, M. R.; Melroy, O. *J. Electroanal. Chem.* **1988**, *239*, 321–331.

(11) Schultze, J. W. In *Proceedings of the II Int. Summer School on Quantum Machanical Aspects of Electrochemistry*, Ohrid, Yugoslavija, 1972.

(12) Schultze, J. W.; Dickertmann, D. *Surf. Sci.* **1976**, *54*, 489–505.

(13) Canon, J. P.; Clavilier, J. *Surf. Sci.* **1984**, *145*, 487–518.

(14) Schultze, J. W.; Dickertmann, D. *Faraday Symp. Chem. Soc.* **1977**, *12*, 36–50.

(15) Schultze, J. W.; Dickertmann, D. *Ber. Bunsenges. Phys. Chem.* **1978**, *82*, 528–534.

(16) Romeo, F. M.; Tucceri, R. I.; Posadas, D. *Surf. Sci.* **1988**, *203*, 186–200.

(17) Takamura, K.; Watanabe, F.; Takamura, T. *Electrochim. Acta* **1981**, *26*, 979–987.

(18) Images were obtained with a NanoscopeII AFM (Digital Instruments, Santa Barbara, CA) operating with a repulsive force between tip and sample of 10^{-9} N. Further experimental details are given in ref 22. AFM experiments were performed in a glove bag under an Ar atmosphere. Solutions contained 1 mM Bi^{3+} and 0.1 M acid and were deoxygenated by Ar prior to use. The substrate was a 65 nm thick film of Au evaporated on mica, and the counter and reference electrodes were an Au wire and an Hg/Hg_2SO_4 electrode, respectively. Potentials are reported relative to the onset of bulk Bi deposition which is 190 ± 5 mV vs NHE in 0.1 M $HClO_4$. Voltammetry was identical with the reported previously.[3,14]

0002-7863/92/1514-5439$03.00/0

Cycling the potential negative of 190 mV causes the (2 × 2)-Bi lattice to disappear and a new ordered rectangular Bi structure to form (Figure 1c). The left side of Figure 1d illustrates the relative positions of the Bi adatoms and the Au(111) substrate. The average spacing between two neighboring Bi adatoms is 0.34 ± 0.02 nm. On the upper left corner of Figure 1d, $\mathbf{P}_1$ and $\mathbf{P}_2$ are vectors forming the primitive unit cell of this lattice. The measured angle between $\mathbf{P}_1$ and $\mathbf{P}_2$ is 94 ± 4°. On the lower left corner of Figure 1d we introduce a nonprimitive unit cell deduced from the spacings and angles in the primitive unit cell as well as the orientation of the overlayer relative to the underlying Au. The nonprimitive cell, given by vectors $\mathbf{U}_1$ and $\mathbf{U}_2$, shows a 0.49 ± 0.03 nm spacing in the direction of $\mathbf{U}_1$ which is $\sqrt{3}$ the Au distance. The rotation of $\mathbf{U}_1$ relative to the Au is 30 ± 3°. In consequence, vector $\mathbf{U}_1$ is commensurate with the [2,1] direction of Au(111). In the $\mathbf{U}_2$ direction, however, a 0.46 ± 0.04 nm spacing is found which is not commensurate with the Au(111) lattice. The Bi structure is then best described as uniaxially commensurate with Au(111). This Bi full monolayer is consistent with the proposed full monolayer structure of Bi on Ag(111) found in a recent X-ray scattering study;[19] however, the Ag(111)/Bi upd system does not exhibit the (2 × 2) open structure.

We observed these structures during both deposition and stripping in the corresponding potential regions and also in solutions containing H_2O_2. We also found the same images and voltammetry in 0.1 M H_2SO_4 and 0.1 M HNO_3 electrolytes, a result which stands in contrast to previous studies of Cu[20,21] and Ag[22] upd on Au(111). This lack of sensitivity toward electrolyte most likely arises from the influence of the considerable partial charge remaining on the Bi adatom in the upd potential region.[9-11] A similar result was found for upd of Hg on Au(111).[23]

The (2 × 2)-Bi structure is observed at the same potentials at which maximum activity for H_2O_2 reduction is found, while both the bare Au(111) and the rectangular lattice are found at potentials where electroreduction activity is substantially less. We thus consider the structural differences between the two inactive lattices and the (2 × 2)-Bi structure. The bare Au surface of course contains no Bi. The rectangular lattice exhibits Bi adatoms, but the packing density of Bi here is substantially greater than that of the 2 × 2 adlattice (64% vs 25% coverage). The (2 × 2)-Bi structure exhibits both open Au and Bi sites, while the rectangular lattice contains almost no open gold sites. Hence, both Au and Bi are required to effect the catalytic reduction of H_2O_2.

The above observation leads to two possible origins of the electrocatalytic activity of the (2 × 2)-Bi lattice. First, H_2O_2 is thought to bind end-on to bare Au[24] giving an Au–O–O intermediate. The end-on binding of H_2O_2 to Au could be enhanced by the presence of Bi, possibly through steric or electronic interactions. Second, the (2 × 2)-Bi lattice could enable the formation of an intermediate wherein H_2O_2 adsorbs on one Au and one Bi atom with a heterobimetallic bridge (Au–O–O–Bi). The peroxide bond length (0.148 nm) is too short to bridge Bi adatoms alone in either the (2 × 2) or rectangular structures. On the surface with the full Bi monolayer, there is not enough open Au fo peroxide to form a bimetallic bridge. A heterobimetallic bound peroxide would polarize the O–O bond and enhance its cleavage, leading to formation of H_2O.

We have shown that two different Bi adlattice structures form during upd of Bi onto Au(111) in acid electrolytes. The (2 × 2)-Bi adlattice exhibits enhanced reactivity toward H_2O_2 reduction relative to the rectangular adlattice because the first structure exhibits both open Bi and Au sites. A heterobimetallic bridge model for H_2O_2 on this surface could explain the enhanced reactivity.

Acknowledgment. C.-h.C. acknowledges a University of Illinois Fellowship in Chemistry. A.A.G. acknowledges a Presidential Young Investigator Award (CHE-90-57953) with matching funds generously provided by Digital Instruments, Inc. This work was funded by the NSF (DMR-89-20538) through the Materials Research Laboratory at the University of Illinois.

(19) Toney, M. F.; Gordon, J. G.; Samant, M. G.; Borges, G. L.; Wiesler, D. G.; Yee, D.; Sorensen, L. B. *Langmuir* **1991**, *7*, 796-802.
(20) Zei, M. S.; Qiao, G.; Lehmpfuhl, G.; Kolb, D. M. *Ber. Bunsenges. Phys. Chem.* **1987**, *91*, 349-353.
(21) Manne, S.; Hansma, P. K.; Massie, J.; Elings, V. B.; Gewirth, A. A. *Science* **1991**, *251*, 183-186.
(22) Chen, C.-H.; Vesecky, S. M.; Gewirth, A. A. *J. Am. Chem. Soc.* **1992**, *114*, 451-458.
(23) Chen, C.-H.; Gewirth, A. A. *Phys. Rev. Lett.* **1992**, *68*, 1571-1574.
(24) Fischer, P.; Heitbaum, J. *J. Electroanal. Chem.* **1980**, *112*, 231-237.

Initial-State and Transition-State Effects on Diels–Alder Reactions in Water and Mixed Aqueous Solvents

Wilfried Blokzijl and Jan B. F. N. Engberts*

Department of Organic Chemistry
University of Groningen, Nijenborgh 4
9747 AG Groningen, The Netherlands

Received March 2, 1992

The fact that rate constants for Diels–Alder (DA) reactions in water are dramatically larger than those in organic solvents[1-11] contradicts with common notion that DA reactions are rather insensitive to solvent effects.[12,13] For example, second-order rate constants for DA reactions[10] of cyclopentadiene (CPD) with methyl vinyl ketone (MVK) and ethyl vinyl ketone (EVK) are enhanced (relative to *n*-hexane) by a factor of ca. 400. The corresponding reaction with naphthoquinones is ca. 6800 times faster.[10] These intriguing solvent effects[14-19] evoked discussions about the molecular origin of this phenomenon. Explanations were sought in terms of high internal solvent pressure,[3,14,15] micellar catalysis,[2a,b] catalysis by hydrogen bonding,[20,21] solvent polarity or solvophobicity effects,[4,6,11] and hydrophobic association.[1f,4,6,11] Some of these explanations are fallacious. First, the internal solvent pressure of water is extremely low[13] and cannot be held

(1) (a) Rideout, D. C.; Breslow, R. *J. Am. Chem. Soc.* **1980**, *102*, 7816. (b) Breslow, R.; Maitra, U.; Rideout, D. *Tetrahedron Lett.* **1983**, *24*, 1901. (c) Breslow, R.; Maitra, U. *Tetrahedron Lett.* **1984**, *25*, 1239. (d) Breslow, R.; Guo, T. *J. Am. Chem. Soc.* **1988**, *110*, 5613. (e) Light, J.; Breslow, R. *Tetrahedron Lett.* **1990**, *31*, 2957. (f) Breslow, R. *Acc. Chem. Res.* **1991**, *24*, 159.
(2) (a) Grieco, P. A.; Yoshida, K.; Garner, P. *J. Org. Chem.* **1983**, *48*, 3139. (b) Grieco, P. A.; Garner, P.; Zhen-min, H. *Tetrahedron Lett.* **1983**, *24*, 1897. (c) Larsen, S. D.; Grieco, P. A. *J. Am. Chem. Soc.* **1985**, *107*, 1768. (d) Grieco, P. A.; Galatsis, P.; Spohn, R. F. *Tetrahedron Lett.* **1986**, *42*, 2847. (e) Grieco, P. A.; Larsen, S.; Fobare, W. F. *Tetrahedron Lett.* **1986**, *27*, 1975.
(3) Lubineau, A.; Quenau, Y. *J. Org. Chem.* **1987**, *52*, 1002.
(4) Schneider, H.-J.; Sangwan, N. K. *J. Chem. Soc., Perkin Trans. 2* **1989**, 1223.
(5) Lattes, A. *J. Chim. Phys. Phys.-Chim. Biol.* **1987**, *84*, 1061.
(6) Cativiela, C.; Garcia, J. I.; Mayoral, J. A.; Avenoza, A.; Pregrina, J. M.; Roy, M. A. *J. Phys. Org. Chem.* **1991**, *4*, 48.
(7) Williams, D. R.; Gaston, R. D.; Horton, I. B. *Tetrahedron Lett.* **1985**, *26*, 1391.
(8) Keana, J. F. W.; Guzikowski, A. P.; Morat, C.; Volwerk, J. J. *J. Org. Chem.* **1983**, *48*, 2661.
(9) (a) Waldmann, H. *Liebigs Ann. Chem.* **1990**, 671. (b) Waldmann, H.; Dräger, M. *Liebigs Ann. Chem.* **1990**, 681.
(10) Blokzijl, W.; Blandamer, M. J.; Engberts, J. B. F. N. *J. Am. Chem. Soc.* **1991**, *113*, 4241.
(11) Hunt, I.; Johnson, C. D. *J. Chem. Soc., Perkin Trans. 2* **1991**, 1051.
(12) Sauer, J.; Sustmann, R. *Angew. Chem., Int. Ed. Engl.* **1980**, *19*, 779.
(13) Reichhardt, C. *Solvents and Solvent Effects in Organic Chemistry*; VCH: Cambridge, 1990.
(14) Grieco, P. A.; Brandess, E. B.; McCann, S.; Clark, J. D. *J. Org. Chem.* **1989**, *54*, 5849.
(15) Lubineau, A.; Meyer, E. *Tetrahedron* **1988**, *44*, 6065.
(16) Kool, E. T.; Breslow, R. *J. Am. Chem. Soc.* **1988**, *110*, 1596.
(17) Laszlo, P.; Lucchetti, J. *Tetrahedron Lett.* **1984**, *25*, 2147.
(18) Luche, J. L.; Petrier, C.; Einhorn, J. *Tetrahedron Lett.* **1985**, *26*, 1449.
(19) Nokami, J.; Otera, J.; Sudo, T.; Okawara, R. *Organometallics* **1983**, *2*, 191.
(20) Kelly, T. R.; Meghani, P.; Ekkundi, V. S. *Tetrahedron Lett.* **1990**, *31*, 3381.
(21) See, for example: Desimoni, G.; Faita, G.; Righetti, P. P.; Toma, L. *Tetrahedron* **1990**, *46*, 7951.

0002-7863/92/1514-5440$03.00/0